Chemistry–A European Journal
Research Article
doi.org/10.1002/chem.202401120
Chemistry Europe
European Chemical Societies Publishing
www.chemeurj.org

Diastereoselective Dearomatizing Cyclizations of 5-Arylpentan-2-ones by Samarium Diiodide – A Computational Analysis

Luca Steiner,*[a, b] Andreas J. Achazi,[c, d] Anne-Marie Kelterer,[b] Beate Paulus,[a] and Hans-Ulrich Reissig*[a]

Dedicated to Prof. Dr. Dr. h. c. mult. Helmut Schwarz

This study analyzes the samarium diiodide-promoted cyclizations of 5-arylpentan-2-ones to dearomatized bicyclic products utilizing density functional theory. The reaction involves a single electron transfer to the carbonyl group, which occurs synchronously with the rate determining cyclization event, and a second subsequent proton-coupled electron transfer. These redox reactions are accurately computed employing small core pseudo potentials explicitly involving all *f*-electrons of samarium. Comparison of the energies of the possible final products rules out thermodynamic control of the observed regio- and diastereoselectivities. Kinetic control via appropriate transition states is correctly predicted, but to obtain reasonable energy levels the influence of the co-solvent hexamethylphosphortriamide has to be estimated by using a correction term. The steric effect of the bulky samarium ligands is decisive for the observed stereoselectivity. Carbonyl groups in *para*-position of the aryl group change the regioselectivity of the cyclization and lead to spiro compounds. The computations suggest again kinetic control of this deviating outcome. However, the standard mechanism has to be modified and the involvement of a complex activated by two SmI_2 moieties is proposed in which two electrons are transferred simultaneously to form the new C–C bond. Computation of model intermediates show the feasibility of this alternative + mechanism.

Introduction

Samarium diiodide – also known as Kagan's reagent – has demonstrated versatile applicability in organic synthesis. Its high chemo-, regio- and stereoselectivity has been exploited in numerous synthetic adventures, including natural product synthesis.[1–10] The easy preparation of homogeneous samarium diiodide solutions in tetrahydrofuran (THF) or other solvents and the fine-tuning of the reagent by addition of salts (e.g. lithium bromide), proton sources (e.g. water, methanol or *tert*-butanol) and strong Lewis bases such as hexamethylphosphortriamide (HMPA) were pivotal for the successful use of this unique electron transfer reagent.[11,12]

Samarium diiodide is particularly important for the diastereoselective formation of new C–C bonds. The coupling of carbonyl groups with a second carbonyl group, an alkenyl or an alkynyl moiety was discovered shortly after Kagan's pioneering contributions. The remarkable reactions of carbonyl groups with arenes as coupling partners lead to synthetically valuable dearomatized products. First singular examples were reported by Schmalz et al. who studied arenes strongly activated by η^6-$Cr(CO)_3$ complexation.[13–15] Starting in 1998, our group systematically investigated SmI_2-promoted cyclizations of simple 5-(het)aryl-2-ones, which efficiently provide polycyclic systems bearing newly formed six-membered rings.[16–24] Recently, You and coworkers reported highly enantioselective versions of such intramolecular carbonyl-arene couplings.[25] Reactions of this type usually require an excess of SmI_2 (> 2 equivalents), whereas catalytic versions operate only in exceptional cases if an auxiliary reducing agent is present.[26–30] This disadvantage weakens the appeal of these transformations for large-scale (industrial) applications.

Very often typical Lewis-basic co-solvents such as HMPA are required in relatively high concentration (usually more than four equivalents with respect to SmI_2). This results in mixtures

[a] L. Steiner, Prof. Dr. B. Paulus, Prof. Dr. H.-U. Reissig
Institut für Chemie und Biochemie
Freie Universität Berlin
Arnimallee 22, 14195 Berlin, Germany
E-mail: Luca.Steiner@fu-berlin.de
hreissig@zedat.fu-berlin.de
[b] L. Steiner, Prof. Dr. A.-M. Kelterer
Institut für Physikalische und Theoretischen Chemie
Technische Universität Graz
Stremayrgasse 9, 8010 Graz, Austria
[c] Dr. A. J. Achazi
Physikalisch-Chemisches Institut
Justus-Liebig-Universität Gießen
Heinrich-Buff-Ring 17, 35392 Gießen, Germany
[d] Dr. A. J. Achazi
Zentrum für Materialforschung
Justus-Liebig-Universität Gießen
Heinrich-Buff-Ring 16, 35392 Gießen, Germany

Supporting information for this article is available on the WWW under https://doi.org/10.1002/chem.202401120

of solvent-separated ion pairs of the type $[Sm(HMPA)_4(THF)_2]I_2$ and $[Sm(HMPA)_6]I_2$ which are characterized by an increased reduction potential of the Sm(II)/Sm(III) redox couple,[31–34] which is essential for many coupling reactions involving carbonyl groups. Unfortunately, HMPA is highly carcinogenic and teratogenic and therefore, less harmful alternatives were developed, which operate at least in certain cases.[35,36] A recent study reports the use of chiral HMPA analogs resulting in highly enantioselective cyclization reactions of indole derivatives, however the generality of this method has still to be demonstrated.[37]

Our broad experimental investigations of the cyclizations of indole derivatives[38–41] were assisted by density functional theory (DFT) calculations which demonstrated the necessity of the incorporation of explicit solvent ligands at the metal center of $SmI_2(THF)_5$.[42] To account for the experimentally observed diastereoselectivity, a chelated complex was proposed where two carbonyl oxygen atoms of the substrate are involved to bind to the samarium center. The influence of HMPA was not considered in this study.

In the current report, we computationally investigate the regio- and diastereoselective cyclizations of 5-arylpentan-2-ones (**1**). Depending on the substituents of the aryl group either annulated bicyclic products **2** or spiro compounds **3** were formed (Scheme 1).[18,21] Similar 5-*exo*-*trig* cyclizations of substrates **1** with strong electron-withdrawing *para*-substituents leading to spiro compounds were reported by Tanaka et al.[43,44] In these reactions two electrons (from Sm(II)) and two protons (from the alcohol) are transferred to the substrate and the overall process can be regarded as an alkylative Birch reaction. Strong Lewis bases such as HMPA are so far inevitable co-solvents in these synthetically valuable cyclizations.

Although mechanisms were proposed for the intriguing reactions of compounds **1**, many important details are still unknown. It is evident that chelate formation is not possible with this type of precursor compounds. We therefore performed DFT-based computations of the involved intermediates, transition states and products in order to identify the rate determining step and the factors that are responsible for the observed regio- and stereoselectivity. The effect of HMPA was taken into account by applying a suitable correction term. The influence of various electron withdrawing and electron donating aryl substituents was also studied in detail and, as a consequence of the computations, an alternative mechanism is discussed for the formation of spiro compounds such as **3**.

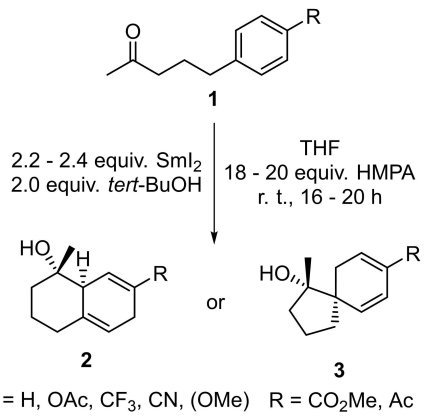

Scheme 1. Diastereoselective dearomatizing cyclizations of 5-arylpentan-2-ones **1** with SmI_2 yielding either annulated bicyclic products **2** or spiro compounds **3** (all formulae in this report represent only the relative configuration of compounds).

Results and Discussion

Energy Profile

The energy profiles for the cyclization reactions of 5-arylpentan-2-ones **1** were computed using the PBE0-D3(BJ)/def2-TZVP//def2-SVP level of DFT, considering THF in the first solvation shell and with a continuum solvation model to mimick the bulk solvent (for details see below). The calculated isodesmic reaction of parent compound **1a** (R = H) with propan-2-ol leading to bicyclic compound **2a** and acetone (Scheme 2) reveals that this process is endergonic (63.2 kJ/mol). This result is not surprising, since an estimation using increments of bond dissociation energies gives a similar value of 60 kJ/mol, showing, that the loss of one of the arene double bonds and of the aromaticity (260 + 150 kJ/mol) is not balanced by the energy gain due to the newly formed C–C bond (−350 kJ/mol). Hence, the contribution of the electron transfer reagent samarium diiodide is decisive to furnish sufficient driving force.

The computational results of the reaction of parent compound **1a** in the presence of $SmI_2(THF)_5$ and methanol leading to the annulated product **2a** are illustrated in detail in Scheme 3. In the very first step, one of the THF ligands of the samarium(II) complex is substituted by precursor **1a** which binds via the oxygen atom of its carbonyl group to deliver primary complex **4a** in an exergonic process (−24.4 kJ/mol). An alternative interaction of the samarium(II) fragment with the phenyl group should be less favorable; the comparable complex of samarium diiodide with toluene is stabilized by only 13.8 kJ/mol (see Supporting Information S1). The Lewis acid/base complex **4a** undergoes an single electron transfer (SET) promoted cyclization via transition state **TS-1** to provide the cyclohexadienyl radical **5a**. *In this step, the configuration of the final product is determined.* The distance between the two carbon atoms of the newly forming C–C bond is 1.85 Å. This relatively short distance and the energy levels of **TS-1** and **5a** indicate that a "late transition state" is involved, which already resembles the structure of the subsequent intermediate. It should be noted that a conceivable samarium ketyl, which was

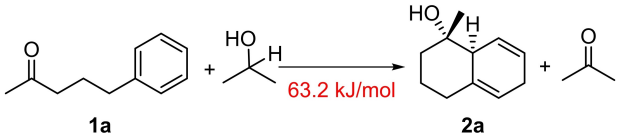

Scheme 2. Isodesmic reaction of parent compound **1a** with propan-2-ol providing **2a** and acetone; the Gibbs free energies were computed using the PBE0-D3(BJ)/def2-TZVP//def2-SVP level of DFT.

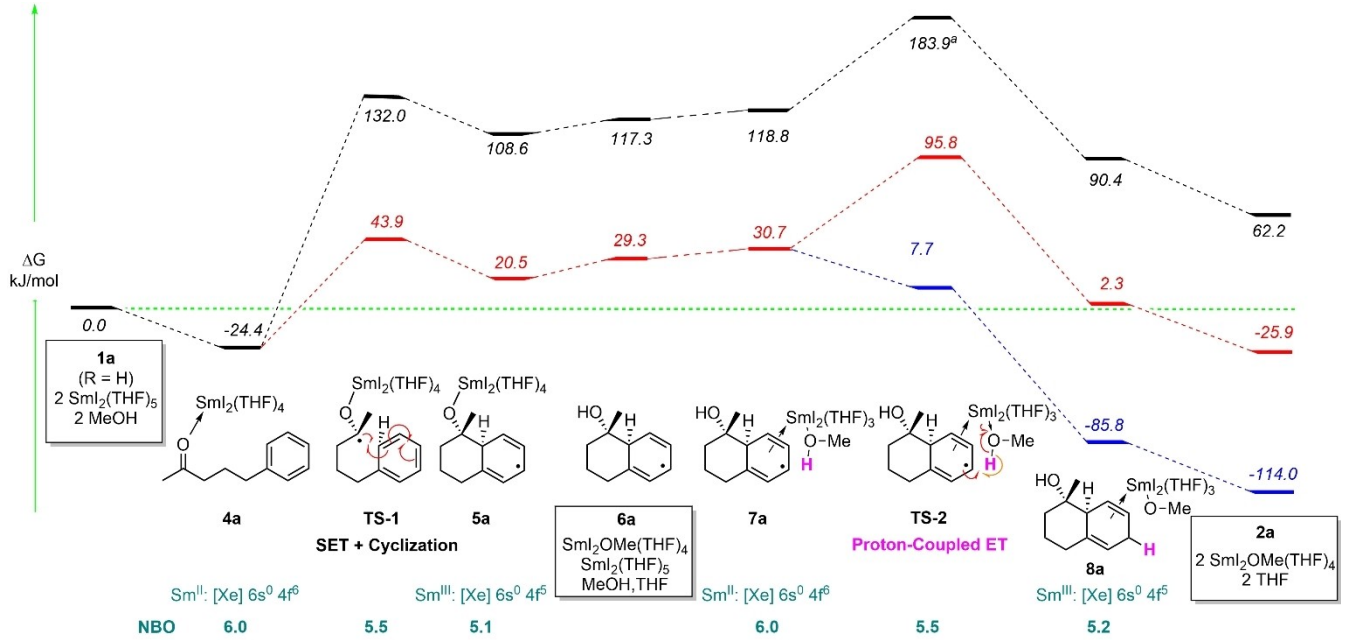

Scheme 3. Energy profile of the samarium diiodide-promoted reaction of 5-phenylpentan-2-one (**1a**) to annulated bicyclic compound **2a**. Gibbs free energies ΔG (in kJ/mol) were computed using the PBE0-D3(BJ)/def2-TZVP//def2-SVP level of DFT. The black numbers refer to the reaction in neat THF; the calculated correction term for HMPA of 88.1 kJ/mol was applied to estimate the influence of this Lewis base on the energies of the involved samarium(III) species (red numbers); this term was applied twice (173.6 kJ/mol) to account for the second Sm(III) in the co-solvent (blue numbers). Natural population analysis occupation numbers of *f*-orbitals are listed to account for the redox state of the involved samarium species. [a]Thermal corrections calculated in gas-phase, see Supporting Information S4.

proposed earlier as intermediate preceding of the cyclization step,[21] is not an intermediate but was assigned as transition state. The inner sphere SET and the cyclization occur rather synchronously according to the calculations.[45] However, the energy level of **TS-1** is very high, as computed in neat THF, which indicates that this reaction is unlikely to proceed at room temperature[46] as experimentally observed in a solution with HMPA as co-solvent. Furthermore, the overall reaction of **4a** to intermediate **5a** via **TS-1** is strongly endergonic (132.0 kJ/mol). These facts demonstrate the necessity to consider HMPA as Lewis-basic ligand at samarium to receive reasonable energy levels (see discussion below).

In order to understand the SET to carbonyl groups, we had earlier computationally investigated the complex of $SmI_2(THF)_4$ with acetone.[47] While the unreduced acetone samarium(II) complex yielded the energy minimum, the corresponding reduced ketyl samarium(III) complex was 84.6 kJ/mol higher in energy, which renders the SET highly endergonic. Reduction of the acetone ligand involves a distortion of the carbonyl group and the geometry of this ketyl species compares surprisingly well to the carbonyl moiety of transition state **TS-1**. Furthermore, both systems show samarium atoms with 5.5 occupied *f*-orbitals according to natural population analysis.[48] From the model study we can conclude that the contribution of the SET is in the order of 85 kJ/mol, hence the additional ca. 71 kJ/mol, which are required to reach **TS-1** from **4a**, originate from the well advanced cyclization event (dearomatization of the arene moiety and moderate ring strain).

The subsequent reaction of intermediate **5a** involves the second SET and protonation. In order to restrict the computational effort, we first replaced the Sm(III) at the oxygen of **5a** by a proton under elimination of $Sm(III)OMe(THF)_4$ to furnish the cyclohexadienyl radical **6a** (center of Scheme 3).[49] This species interacts further with the second equivalent of $Sm(II)I_2(THF)_5$ and methanol to provide a complex with the pentadienyl subunit of the bicyclic system providing intermediate **7a** which also includes methanol as ligand.[50] Two diastereomeric complexes are possible, but only the sterically more favorable diastereomer **7a** was considered in this Scheme. The samarium fragment is on the side of the bridgehead hydrogen and hence on the sterically better accessible convex face of bicyclic intermediate **6a**. The samarium center is located essentially on top of a C–C double bond of the pentadienyl subunit as shown in Figure 1. In addition, the proton source methanol is activated

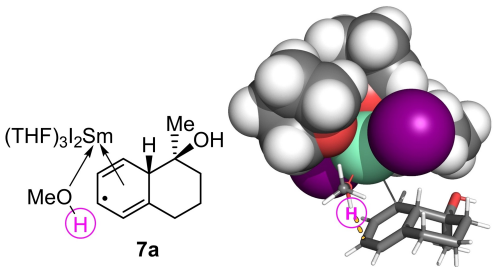

Figure 1. Optimized calculated structure of complex **7a** with $SmI_2(TFH)_3MeOH$ computed at the PBE0-D3(BJ)/def2-TZVP//def2-SVP level of DFT; (color code, samarium: turquoise, iodide: purple, oxygen: red).

and pre-orientated by the complexation with samarium(II).[51] This arrangement facilitates the subsequent regioselective proton-coupled electron transfer (PCET) via **TS-2** affording the new complex **8a**.[52–54] The barrier of this step is considerably lower (65.1 kJ/mol) compared to **TS-1**. The reaction from **7a** to **8a** is exergonic (−28.4 kJ/mol), however the involved species are still energetically quite unfavorable. The decomplexation under ejection of $Sm(III)(THF)_4OMe$ gives the final product **2a**, again in an exergonic process (−28.2 kJ/mol).[55] Overall, the energy profile of the reaction shown in Scheme 3 (black numbers) reveals that the complete process is endergonic in THF. The value of 62.2 kJ/mol approximately coincidences with the value obtained by the calculated isodesmic reaction (Scheme 2) and hence the electron transfer due to oxidation of the involved Sm(II) species to Sm(III) does not contribute to the driving force of the process.[56] As a consequence, it is inevitable to take into account the so far neglected co-solvent HMPA.

Explicit consideration of HMPA ligands at samarium is computationally very demanding for complex reactions such as **1a** to **2a**. Hence, we rely on experimental and computational data obtained from model reactions in the presence of HMPA. They reveal that a high stabilization of the oxidized stage is responsible for the effect of this powerful Lewis base, certainly caused by the pronounced oxophilicity of samarium(III). By measuring the reduction potentials of SmI_2 it was found that four equivalents of HMPA raise the reduction potential by 69.2 kJ/mol (0.72 eV)[32,33] or even by 86.8 kJ/mol (0.90 eV).[31,34] The latter value agrees very well with the results of our model study with acetone and SmI_2 with either four molecules of THF or HMPA in the first solvation shell in bulk THF.[47] The calculated ionization potential of the complex was reduced by 88.1 kJ/mol (applying Koopman's theorem) when the THF ligands were replaced by HMPA. While HMPA thus very strongly influences the thermodynamics, its kinetic effects are weaker.[31,52–54] The reported rate accelerations translate to a correction term of approximately 20 kJ/mol according to Arrhenius' law.[31] This value also agrees very well with the reported value from computations of 21 kJ/mol.[47] However, the reported kinetic studies do not involve any reactions under dearomatization, which causes the discussed late transition state. Therefore, **TS-1** is structurally and energetically well comparable to intermediate **5a** and as a consequence it is expedient to consider the thermodynamic effect of HMPA.

If we accept the calculated value of 88.1 kJ/mol as correction term, the energies of **TS-1**, **5a**, **6a**, and **7a** were strongly reduced (Scheme 3, red numbers). With these lower energy levels, the formation of the cyclohexadienyl radical **5a** becomes only moderately endergonic and the barrier via **TS-1** is compatible with a reaction occurring at room temperature. Applying this correction for the subsequent steps, the overall reaction to **2a** becomes exergonic (−25.9 kJ/mol). Furthermore, if the correction term is used twice for species where the second equivalent of samarium(III) is involved, i.e. starting with **TS-2**, the barrier of the PCET to intermediate **8a** is strongly decreased (Scheme 3, blue numbers). Although this approach may overestimate the effect of HMPA, in particular concerning the energies of the transition states, it shows that the overall process now becomes kinetically and thermodynamically feasible.

The calculation of the energy profile without consideration of HMPA showed that a samarium ketyl is not an intermediate but a transition state (**TS-1** of Scheme 3) and that the SET occurs simultaneously with the cyclization event. Does HMPA as ligand fundamentally change this prediction? Although we did not compute the transition state our model study with acetone as substrate indicates that this is not the case.[47] The calculated samarium(III) ketyl is not an energy minimum, regardless whether it is coordinated by four THF or by four HMPA ligands. Furthermore, the geometries of these two species are very similar (with slightly longer samarium oxygen bond in the presence of HMPA). Since the calculated transition state **TS-1** is structurally very similar to that of this model system with THF ligands we can assume with high fidelity that this is also valid for HMPA (for a detailed comparison, see Supporting Information S3). Hence, the samarium ketyl is not an intermediate but a transient stage of the process – even in the presence of HMPA.

Diastereoselectivity

The samarium diiodide-promoted reaction of precursor **1a** provided only diastereomer **2a**.[21] We can rule out thermodynamic control of the observed diastereoselectivity by comparing the Gibbs free energies of **2a** with the conceivable isomer **2a'** (Scheme 4) which is even slightly more stable than the exclusively isolated product **2a**. As mentioned above, the diastereoselectivity of the overall reaction is determined by the C–C bond forming step involving transition state **TS-1**. The computations reveal that its diastereomorphic counterpart **TS-1'** is 10.8 kJ/mol higher in energy. This energy difference is probably even too low since the very bulky HMPA ligands at the samarium center are neglected. After formation of the new C–C bond the energy differences of the diastereomeric

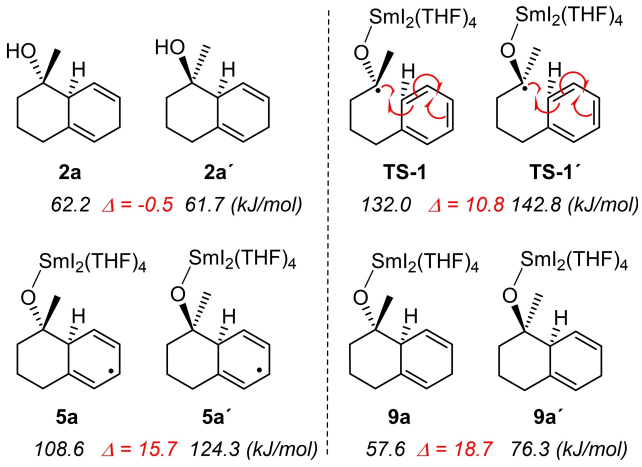

Scheme 4. Comparison of products **2a**/**2a'**, of diastereomorphic transition states **TS-1**/**TS-1'** and of diastereomeric intermediates **5a**/**5a'** and **9a**/**9a'** (all Gibbs free energies were computed at the PBE0-D3(BJ)/def2-TZVP//def2-SVP level of DFT).

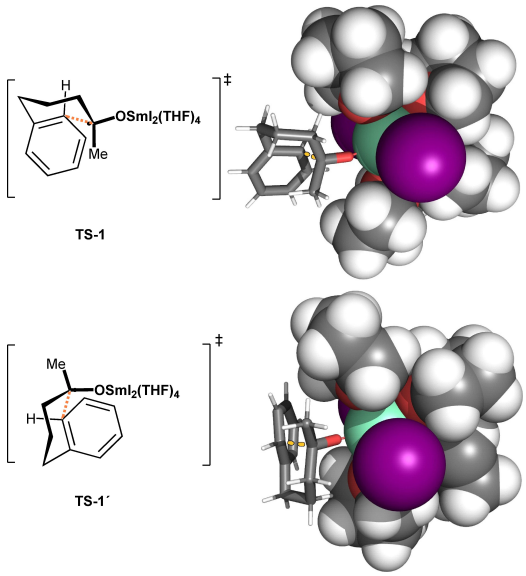

Figure 2. Lewis structures of diastereomorphic transition states **TS-1** and **TS-1'** along with their PBE0-D3(BJ)/def2-TZVP optimized structures (the space filling structures are based on the van der Waal radii; color code, samarium: turquoise, iodide: purple, oxygen: red).

intermediates **5a**/**5a'** and **9a**/**9a'** are even slightly higher possibly due to the shorter fully established C–C bond.

The geometries of the two transition states are presented in Figure 2 which also depicts two Lewis structures earlier proposed to rationalize the experimentally observed result.[18,21] Two chair-like arrangements are possible and the preferred transition state (corresponding to **TS-1**) avoids repulsive penalties, since the benzene moiety of the forming intermediate points away from the bulky samarium complex. The positioning of this fragment in the alternative transition state **TS-1'** causes unfavorable interactions. These are apparent when the computed space filling structures of Figure 2 are inspected. The $SmI_2(THF)_3$ moiety of **TS-1'** is forced into very close proximity to the newly forming bicyclic part of the intermediate. The calculated distances of the *para*-carbon atom of the arene ring to the samarium center is 4.97 Å for **TS-1'** compared to 5.75 Å in **TS-1**; the distances of this carbon to the oxygen amount to 3.51 Å versus 4.13 Å, clearly showing that **TS-1'** is severely more crowded than **TS-1**.

Influence of Substituents and Regioselectivity

Most of the cyclization reactions under discussion proceed to form the annulated bicyclic products **2** (Scheme 1). However, an interesting exception was found when strongly electron-withdrawing carbonyl groups were present in *para*-position of the aryl group. Then, an *ipso*-attack and the formation of spiro compounds **3** was observed.[21,43,44] This 5-*exo*-*trig* cyclization is an allowed process according to Baldwin's rules.[57] In Table 1, we compare the energies of the annulated bicyclic standard products **2** with that of the corresponding spiro compounds **3** for two typical examples (**a**: R = H and **b**: R = CO_2Me). Remarkably, for both systems the bicyclic annulated products were found to be ca. 37 kJ/mol more stable than the corresponding spiro compounds, although in the case of precursor **1b** only the compound **3b** was isolated. We attribute this energy difference to the ring strain of spiro compounds **3** and the additional unfavorable gauche interactions of substituents attached to the five-membered ring.[58] These effects should be independent of the substituents in the cyclohexadiene substructure of **3**. From these data, we can conclude that the formation of spiro compounds should be a kinetically controlled process.

Table 1. Gibbs free energies (in kJ/mol) of annulated bicyclic products **2** and the corresponding spiro compounds **3** (computed at the PBE0-D3/def2-TZVP//def2-SVP level of DFT).

Substituent R	Annulated Product **2**	Spiro Compound **3**	Experimental Result
H	62.2	99.1	**2a** (**3a** not found)
CO_2Me	55.7	92.2	**3b** (**2b** not found)

The calculated transition state **TS-4** of the reaction of precursor **1b** with samarium diiodide leading to **3b** lies 28 kJ/mol higher than **TS-3**, which means that the unobserved product **2b** should be formed (Scheme 5). Comparison of the subsequent intermediates **10b** and **5b** and that of the protonated intermediates **11b** and **6b**, respectively, reveal energy differences in a similar order. This demonstrates again that the transition states of the cyclization are "late" and resemble the subsequent intermediates. However, kinetic control leading to the observed product cannot be deduced

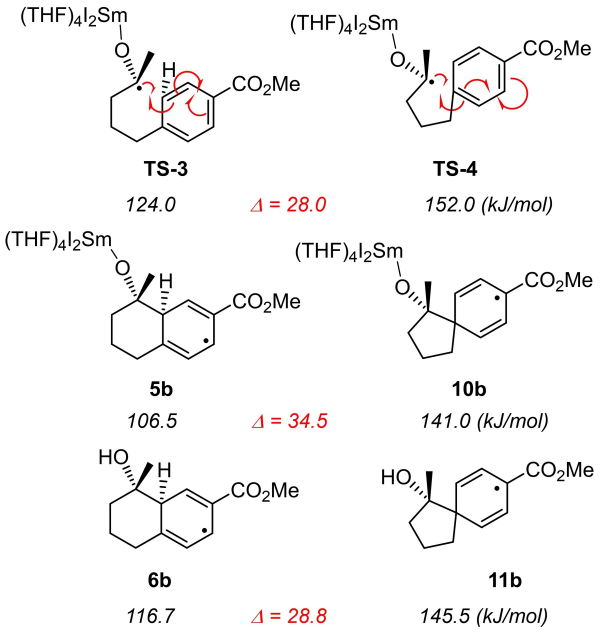

Scheme 5. Comparison of transition states **TS-3**/**TS-4** and of intermediates **5b**/**10b**, and **6b**/**11b** (all Gibbs energies were computed at the PBE0-D3(BJ)/def2-TZVP//def2-SVP level of DFT).

from these numbers. *Instead, an alternative mechanistic scenario has to be developed to explain the formation of spiro compounds.*

Before discussing an alternative mechanism, the energies of differently substituted intermediates **5** and **10** are compared (Scheme 6). The computed energy of **5a** (R = H, see Scheme 3) is supplemented by that of the conceivable spiro intermediate **10a** which lies 54.7 kJ/mol higher. The energies of **5b** and **10b** ($R = CO_2Me$) differ in 34.5 kJ/mol while the cyano-substituted intermediates **5c** and **10c** show a similar difference of Gibbs free energies. Interestingly, the trifluoromethyl-substituted species **5d** and **10d** reveal a stronger preference for the annulated intermediate **5d**, which is energetically favored by 46.5 kJ/mol. At this point, it should be noted that a radical in intermediates **10b** and **10c** should be stabilized by their electron-withdrawing substituents in comparison with R = H, whereas the role of a CF_3 group is ambivalent. The calculated energy of the *para*-methoxy-substituted annulated radical intermediate **5e** lies considerably higher than those of **5a**–**5d**. The electron-donating methoxy group apparently destabilizes this intermediate (and the preceding transition state), which is in accordance with the experimental observation that precursor **1e** does not cyclize cleanly to **2e**.[21] The spiro intermediate **10e** is even less stable by ca. 32 kJ/mol.

The trend of energy differences between annulated and spiro intermediates **5** and **10**, respectively, roughly corresponds to the stabilizations of C-centered radicals by the substituents, showing ca. 35 kJ/mol for CO_2Me, CN and OMe, whereas a trifluoromethyl substituent exhibits a moderate destabilization of 6 kJ/mol (see green numbers in the right part of Scheme 6).[59] It is evident from this analysis that the stabilization of the radicals by the substituents is not sufficient to allow the formation of the spiro intermediates **10**. Also, there is a striking similarity of the values in series **5b**/**10b** and **5c**/**10c** which does not reflect at all the experimental differences. The methoxycarbonyl-substituted system provides the spiro compound **3b** whilst the cyano-substituted system behaves "normally" and delivers the annulated product **2c**.[18,21]

What is the mechanistic alternative? We suggest that the arene substituent of **1b** undergoes a primary interaction with the oxophilic samarium diiodide, which is not operating with a cyano group.[60] Although the calculated complex **12b** is 8.3 kJ/mol higher in energy than the corresponding complex **4b**,[61] where $SmI_2(THF)_4$ binds to the oxygen of the keto group (Scheme 7), the interaction of this substituent with samarium diiodide may play the decisive role for this reaction. This Lewis acid/base complexation further increases the electron-withdrawing nature of the methoxycarbonyl group.[62]

The subsequent cyclization may therefore start with the doubly-activated complex **13b** and via transition state **TS-5** two electrons are shifted furnishing intermediate **14b**. Whether the two electrons are transferred simultaneously or stepwise cannot be decided since the system is too large for DFT calculations at appropriate level. The final protonations at the cyclohexadiene moiety and at the oxygen by the present methanol complete the reaction sequence. It is remarkable that the C-protonation in the six-membered ring proceeds not only regioselectively but also stereoselectively providing the diastereomer of **3b** as drawn. Interestingly, the proton is attached to the side of **14b**, which is in proximity to the samariumoxy part. We can therefore speculate that the proton is steered due to the attachment of the alcohol to the samarium similar to the arrangement in complex **7a** (Figure 1).

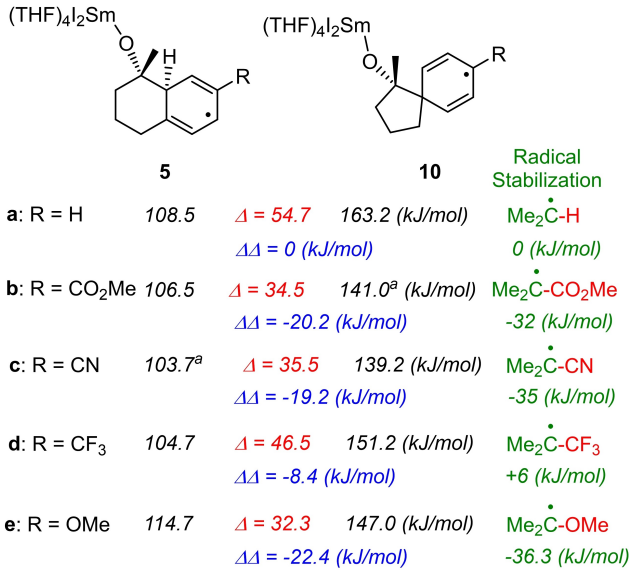

Scheme 6. Comparison of the Gibbs free energies of annulated intermediates **5a**–**e** with those of the spiro intermediates **10a**–**e** (computed at the PBE0-D3(BJ)/def2-TZVP//def2-SVP level of DFT; the blue ΔΔ values are the difference of the red Δ values relative to **5a**) and literature reported radical stabilization energies[59] of substituents (green numbers).[a] Enlarged differential increment, see Supporting Information S4.

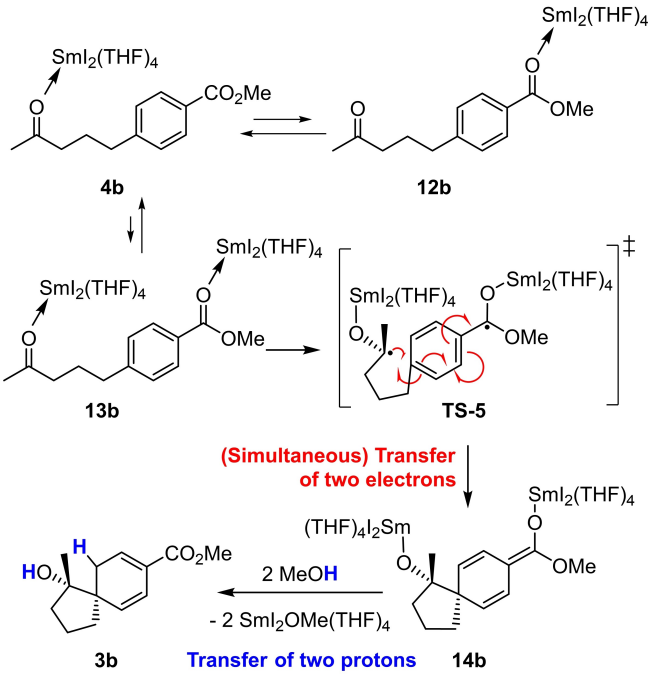

Scheme 7. Alternative mechanism for the formation of spiro compound **3b** with doubly-activated complex **13b**, **TS-5** and intermediate **14b** as crucial species.

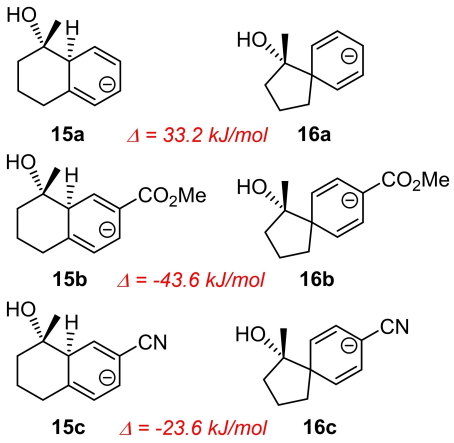

Scheme 8. Comparison of the Gibbs free energies of anionic annulated intermediates **15a–c** with those of anionic spiro intermediates **16a–c** (computed at the PBE0-D3(BJ)/def2-TZVP//def2-SVP level of DFT).

Considerably simplifying, intermediate **14b** can be regarded as an anionic species with a samarium(III) as counter cation. In order to estimate the stability of this kind of species, we compared the Gibbs free energies of the annulated pentadienyl anions **15a–c** and the corresponding spiro intermediates **16a–c** (Scheme 8). For the parent system, anion **15a** is favored over the spiro system **16a** – as mentioned, strain effects are probably responsible for this difference. Not surprisingly, the ability of a methoxycarbonyl group to stabilize a negative charge results now in a preference for the spiro intermediate **16b**. This effect is less pronounced for the cyano-substituted species **16c**. Comparison of these stabilization energies support our interpretation that only the strongly electron-withdrawing CO_2Me group (and the electronically similar COMe group) steer the cyclization to spiro compounds **3**, whereas all other substituents lead to the "normal" annulated products **2**. The particular role of the complexation of samarium(II) to the oxygen of the carbonyl groups, which is not possible for the cyano substituent, has already been mentioned.

It has been experimentally shown, that the reaction of **1b** with samarium diiodide can be performed in the absence of proton sources under trapping of the intermediate corresponding to **14b** (and to simplified structure **16b**) by electrophiles such as allyl bromide.[44] This apparently longer life time of the anionic intermediate strongly supports the suggested alternative reaction mechanism.

Conclusions

The mechanisms of the samarium diiodide-promoted cyclizations of 5-arylpentan-2-ones **1** to bicyclic compounds **2** or **3** are correctly predicted by DFT calculations, which involve all *f*-electrons of samarium. The parent system **1a** provides the annulated bicyclic product **2a** via a stepwise process, first involving an electron transfer from samarium(II) to the carbonyl group, which occurs synchronously with the decisive cyclization step. This rate determining step also constitutes the relative configuration of the final product. The calculated transition state **TS-1** correctly predicts the observed diastereoselectivity, the alternative transition state **TS-1'** suffers severe steric interactions due to the bulky samarium-ligand moiety. A proton coupled second electron transfer finally leads to the isolated product **2a**. The influence of the essential co-solvent HMPA was estimated by using a correction term derived from a computational model study. This term reflects the high stabilization of the oxophilic samarium(III) by the Lewis basic HMPA ligands. The procedure allows a correction of the energy profile of the overall reaction and makes all steps thermodynamically and kinetically feasible. The calculations reveal that the involved samarium ketyl species is not an intermediate as earlier proposed but a transition state with already well advanced cyclization event. It was proposed that this scenario is also valid in the presence of HMPA. Overall, the DFT calculations are in good agreement with the earlier proposed mechanistic scenario with a "carbonyl first"[63] activation to start the multi-step process.

On the other hand, the computational results show that this standard pathway is not applicable to the reaction of *para*-methoxycarbonyl-substituted derivative **1b**. Thermodynamics and kinetics favor the formation of the annulated product **2b** which is experimentally not observed. Therefore, an alternative mechanism was developed, which involves a complex **13b** where both carbonyl groups are activated by two samarium diiodide molecules. This crucial doubly-activated precursor undergoes the cyclization by transfer of two electrons, which may occur simultaneously or stepwise. The calculations of simplified anionic species such as **16b** made this modified pathway very likely. This "both carbonyl first" mechanism is related to the proposed double-activation of electron-deficient indole derivatives[39] for which DFT calculations suggest a geometrically possible chelate involving only one $SmI_2(THF)_3$ unit before electron transfer and cyclization.

In summary, the many mechanistic details obtained in this study showed the power of DFT calculations – even if lanthanoids such as samarium are involved in complex reactions. The key was to explicitly include all *f*-electrons of samarium and to derive a suitable approximation to account for the effect of HMPA.[64] On this basis, the development of new dearomatizing transformations[65] or of catalytic versions of samarium diiodide-promoted reactions may be possible.

Computational Methodology

We performed unrestricted single reference density functional theory (DFT) calculations using the TURBOMOLE 7.3 program package.[66] The electronic energies were computed at optimized geometric structures employing the PBE0-D3(BJ) functional[67–71] with the def2-TZVP[72] basis set and corresponding ECP28MWB (I, Sm) effective core potential. The COSMO[73,74] model was applied for implicit solvation, with a dielectric constant (ε) of 7.4, representing THF as the solvent. The integration of the exchange correlation functional was carried out using the multigrid *m4*. To improve the initial wave function guess, thermal smearing of electrons was applied, with a starting temperature of 400 K and appropriate high-spin multiplicity constraints. The resolution of identity approxima-

tion was applied with the corresponding auxiliary basis set for density fitting. The SCF energy convergence threshold was set to 10^{-6} atomic units (au), and gradients were converged to 10^{-3} au for electronic energies.

For thermal corrections at 1 bar and 298.15 K, geometric structures were converged with def2-SVP basis set utilizing the computational details mentioned earlier until the gradient change was smaller than 10^{-4} au and the SCF energy convergence was smaller than 10^{-8} au. Numerical calculation of the Hessian was performed with inclusion of derivatives of the quadrature weights and a constant damping factor of 0.7 as Pulay mixing coefficient. In contrast to the standard entropy calculation, we additionally utilized Grimme's quasi-RRHO approximation for frequencies lower than 100 cm^{-1}.[75]

Transition states searches were performed by scanning the reaction coordinate until the gradient threshold of $< 5\times10^{-4}$ au was attained for the highest point in energy. The resulting distance was then used in a constrained def2-TZVP optimization to derive electronic energies. All saddle points exhibited exactly one imaginary frequency, while minimum geometric structures were verified to have only positive frequencies.

Supporting Information

The authors have cited additional references within the Supporting Information.

Acknowledgements

The authors would like to thank the HPC Service of ZEDAT, Freie Universität Berlin, for the computing time. Open Access funding enabled and organized by Projekt DEAL.

Conflict of Interests

The authors declare no conflict of interest.

Data Availability Statement

The data that support the findings of this study are available in the supplementary material of this article.

Keywords: dearomatization reaction · density functional theory · electron transfer · hexamethylphosphortriamide · samarium

[1] P. Girard, J. Namy, H. Kagan, *J. Am. Chem. Soc.* **1980**, *102*, 2693–2698.
[2] G. A. Molander, C. R. Harris, *Chem. Rev.* **1996**, *96*, 307–338.
[3] D. J. Edmonds, D. Johnston, D. J. Procter, *Chem. Rev.* **2004**, *104*, 3371–3340.
[4] D. J. Procter, R. A. Flowers, T. Skrydstrup, *Organic synthesis using samarium diiodide*, Royal Society of Chemistry **2010**.
[5] C. Beemelmanns, H.-U. Reissig, *Chem. Soc. Rev.* **2011**, *40*, 2199–2210.
[6] M. Szostak, M. Spain, D. J. Procter, *Chem. Soc. Rev.* **2013**, *42*, 9155–9183.
[7] M. Szostak, N. J. Fazakerley, D. Parmar, D. J. Procter, *Chem. Rev.* **2014**, *114*, 5959–6039.
[8] J. Gong, H. Chen, X.-Y. Liu, Z.-X. Wang, W. Nie, Y. Qin, *Nat. Commun.* **2016**, *7*, 12183–12188.
[9] J. C. Leung, A. A. Bedermann, J. T. Njardarson, D. A. Spiegel, G. K. Murphy, N. Hama, B. M. Twenter, P. Dong, T. Shirahata, I. M. McDonald, M. Inoue, N. Taniguchi, T. C. McMahon, C. M. Schneider, N. Tao, B. M. Stoltz, J. L. Wood, *Angew. Chem.* **2018**, *130*, 2009–2012; *Angew. Chem. Int. Ed.* **2018**, *57*, 1991–1994.
[10] Y. Ashida, K. Arashiba, K. Nakajima, Y. Nishibayashi, *Nature* **2019**, *568*, 536–540.
[11] K. Otsubo, J. Inanaga, M. Yamaguchi, *Tetrahedron Lett.* **1986**, *27*, 5763–5764.
[12] J. Inanaga, M. Ishikawa, M. Yamaguchi, *Chem. Lett.* **1987**, *16*, 1485–1486.
[13] H.-G. Schmalz, S. Siegel, J. W. Bats, *Angew. Chem.* **1995**, *107*, 2597–2599; *Angew. Chem. Int. Ed. Engl.* **1995**, *34*, 2383–2385.
[14] H.-G. Schmalz, S. Siegel, A. Schwarz, *Tetrahedron Lett.* **1996**, *37*, 2947–2950.
[15] H.-G. Schmalz, C. B. de Koning, D. Bernicke, S. Siegel, A. Pfletschinger, *Angew. Chem.* **1999**, *111*, 1721–724; *Angew. Chem. Int. Ed.* **1999**, *38*, 1620–1623.
[16] C. U. Dinesh, H.-U. Reissig, *Angew. Chem.* **1999**, *111*, 874–876; *Angew. Chem. Int. Ed.* **1999**, *38*, 789–791.
[17] E. Nandanan, C. U. Dinesh, H.-U. Reissig, *Tetrahedron* **2000**, *56*, 4267–4277.
[18] M. Berndt, H.-U. Reissig, *Synlett* **2001**, 1290–1292.
[19] F. Aulenta, M. Berndt, I. Brüdgam, H. Hartl, S. Sörgel, H.-U. Reissig, *Chem. Eur. J.* **2007**, *13*, 6047–6062.
[20] U. K. Wefelscheid, H.-U. Reissig, *Adv. Synth. Catal.* **2008**, *350*, 65–69.
[21] U. K. Wefelscheid, M. Berndt, H.-U. Reissig, *Eur. J. Org. Chem.* **2008**, 3635–3646.
[22] H.-U. Reissig, A. Niermann, *Synlett* **2011**, 525–528.
[23] C. N. Rao, D. Lentz, H.-U. Reissig, *Angew. Chem.* **2015**, *127*, 2788–2792; *Angew. Chem. Int. Ed.* **2015**, *54*, 2750–2753.
[24] Review on initial work: M. Berndt, S. Gross, A. Hölemann, H.-U. Reissig, *Synlett* **2004**, 422–438.
[25] Y. Wang, W.-Y. Zhang, Z.-L. Yu, C. Zheng, S.-L. You, *Nat. Synth.* **2022**, *1*, 401–406.
[26] F. Hélion, J.-L. Namy, *J. Org. Chem.* **1999**, *64*, 2944–2946.
[27] H. C. Aspinall, N. Greeves, C. Valla, *Org. Lett.* **2005**, *7*, 1919–1922.
[28] S. Maity, R. A. Flowers II, *J. Am. Chem. Soc.* **2019**, *141*, 3207–3216.
[29] S. Maity, *Eur. J. Org. Chem.* **2021**, 5312–5319.
[30] a) S. Agasti, N. A. Beattie, J. J. W. McDouall, D. J. Procter, *J. Am. Chem. Soc.* **2021**, *143*, 3655–3661; b) S. Agasti, F. Beltran, E. Pye, N. Kaltsoyannis, G. E. M. Crisenza, D. J. Procter, *Nat. Chem.* **2023**, *15*, 535–541.
[31] R. J. Enemærke, T. Hertz, T. Skrydstrup, K. Daasbjerg, *Chem. Eur. J.* **2000**, *6*, 3747–3754.
[32] M. Shabangi, R. A. Flowers II, *Tetrahedron Lett.* **1997**, *38*, 1137–1140.
[33] M. Shabangi, M. L. Kuhlman, R. A. Flowers II, *Org. Lett.* **1999**, *1*, 2133–2135.
[34] R. J. Enemærke, K. Daasbjerg, T. Skrydstrup, *Chem. Commun.* **1999**, 343–344.
[35] a) C. McDonald, J. D. Ramsey, D. G. Sampsell, J. A. Butler, M. R. Cecchini, *Org. Lett.* **2010**, *12*, 5178–5181; b) M. Berndt, A. Hölemann, A. Niermann, C. Bentz, R. Zimmer, H.-U. Reissig, *Eur. J. Org. Chem.* **2012**, 1299–1302.
[36] C. N. Rao, H.-U. Reissig, *Eur. J. Org. Chem.* **2021**, 6392–6399.
[37] W.-Y. Zhang, H.-C. Wang, Y. Wang, C. Zheng, S.-L. You, *J. Am. Chem. Soc.* **2023**, *145*, 10314–10321.
[38] S. Gross, H.-U. Reissig, *Org. Lett.* **2003**, *5*, 4305–4307.
[39] C. Beemelmanns, V. Blot, S. Gross, D. Lentz, H.-U. Reissig, *Eur. J. Org. Chem.* **2010**, 2716–2732.
[40] C. Beemelmanns, H.-U. Reissig, *Angew. Chem.* **2010**, *122*, 8195–8199; *Angew. Chem. Int. Ed.* **2010**, *49*, 8021–8025.
[41] C. Beemelmanns, H.-U. Reissig, *Chem. Rec.* **2015**, *15*, 872–885.
[42] A. J. Achazi, D. Andrae, H.-U. Reissig, B. Paulus, *J. Comput. Chem.* **2017**, *38*, 2693–2700.
[43] H. Ohno, S.-i. Maeda, M. Okumura, R. Wakayama, T. Tanaka, *Chem. Commun.* **2002**, 316–317.
[44] H. Ohno, M. Okumura, S.-i. Maeda, H. Iwasaki, R. Wakayama, T. Tanaka, *J. Org. Chem.* **2003**, *68*, 7722–7732.
[45] According to DFT calculations of Procter et al. (see ref. 30b) on samarium diiodide catalyzed cycloadditions of bicyclo[1.1.1]pentyl-substituted ketones the involved samarium ketyl was found to be transient stage and not an intermediate.
[46] H. Ryu, J. Park, H. K. Kim, J. Y. Park, S.-T. Kim, M.-H. Baik, *Organometallics* **2018**, *37*, 3228–3239.

[47] L. Steiner, A. J. Achazi, B. Vlaisavljevich, P. Miro, B. Paulus, A.-M. Kelterer, *Molecules* **2022**, *27*, No. 8673.
[48] Another source of uncertainty is the energetic contribution of the spin orbit coupling (SOC) which is a frequent topic in computations of redox reactions of lanthanoids (see: a) C. E. Kefalidis, L. Perrin, L. Maron, *Eur. J. Inorg. Chem.* **2013**, 4042–4049; b) Review: C. E. Kefalidis, L. Castro, L. Perrin, I. Del Rosal, L. Maron, *Chem. Soc. Rev.* **2016**, *45*, 2516–2543). The magnitude of the SOC is quantified by a pseudo-potential based approach (see Supporting Information S3) showing that the change of barrier is lower than 4 kJ/mol and thus negligible in the present discussion.
[49] In the experiments (Scheme 1), *tert*-butanol was used as proton source and therefore the reaction of **5a** with this more bulky alcohol was also calculated. A destabilization of 5.3 kJ/mol was found which compares well to the value of 8.5 kJ/mol for the destabilization during the reaction of **5a** with methanol to **6a**. The proton source hence has only a very limited influence on the energies and therefore we continued our calculations with methanol, which is computationally easier to handle.
[50] When intermediate **7a** forms, two states can arise with either sextet or octet spin multiplicity, depending on whether the radical site of **6a** opposes or aligns with the spin of the septet of $SmI_2(THF)_5$. While the sextet and octet states are close in energy we used the 2.7 kJ/mol less stable sextet state since only this state offers a spin-conserving reaction pathway.
[51] G. Boekell, R. A. Flowers II, *Chem. Rev.* **2022**, *122*, 13447–13477.
[52] E. Prasad, R. A. Flowers II, *J. Am. Chem. Soc.* **2002**, *124*, 6895–6899.
[53] E. Prasad, B. W. Knettle, R. A. Flowers II, *J. Am. Chem. Soc.* **2004**, *126*, 6891–6894.
[54] D. V. Sadasivam, P. K. S. Antharjanam, E. Prasad, R. A. Flowers II, *J. Am. Chem. Soc.* **2008**, *130*, 7228–7229.
[55] In a model study, we performed experiments in the presence of *tert*-BuOD which showed incomplete deuterium incorporation. This was interpreted as hydrogen abstraction from the solvent THF (Andre Niermann, Dissertation, Freie Universität Berlin, 2012). Nevertheless, we conclude that the main pathway of the reaction involves intermediates as illustrated in Scheme 2.
[56] This fact is supported by the calculation of the redox reaction of acetone with two equivalents of $SmI_2(THF)_5$ and methanol to isopropanol and the corresponding samarium(III) species. The Gibbs free energy of −1.0 kJ/mol shows that this reaction is essentially thermoneutral.
[57] a) J. E. Baldwin, *J. Chem. Soc. Chem. Commun.* **1976**, 734–736; b) I. V. Alabugin, K. Gilmore, *Chem. Commun.* **2013**, *49*, 11246–11250.
[58] The energy difference of the parent skeletons of **2** (1,2,3,4,4a,7-hexahydronaphthalene) and **3** (spiro[4.5]deca-6,8-diene) amounts to 29.1 kJ/mol and hence the repulsive interaction due to the two substituents is ca. 8 kJ/mol.
[59] a) H. Zipse, *Top. Curr. Chem.* **2006**, *263*, 163–189; b) J. Hioe, H. Zipse, *Radical Stability – Thermochemical Aspects in Encyclopedia of Radicals in Chemistry, Biology and Materials* Vol 1 (Eds.: C. Chatgilialoglu, A. Studer), John Wiley & Sons, New York, **2012**, pp. 449–475.
[60] For attempts to quantify the interaction of alcohols and amines with samarium diiodide: a) S. De, S. Hoz, *J. Org. Chem.* **2021**, *86*, 10861–10865; b) A. Ramírez-Solís, N. G. Boekell, C. I. León-Pimentel, H. Saint-Martin, C. O. Bartulovich, R. A. Flowers II, *J. Org. Chem.* **2022**, *87*, 1689–1697.
[61] This difference corresponds to the lower proton affinity of ethyl benzoate compared to acetone. See, E. P. L. Hunter, S. G. Lias, *J. Phys. Chem.* **1998**, *27*, 413–656.
[62] Complexes similar to **12b** or **13b** are not possible for the parent compound **1a**. However, we can speculate that a complex of $SmI_2(THF)_x$ with its arene ring may be possible (as with the model compound toluene) and that this may cause a similar, but weaker activation of the aryl group for an attack of the carbonyl group. This would resemble the systems studied by Schmalz et al. with $Cr(CO)_3$-activated arenes (see ref. 14, 15). Unfortunately, the corresponding doubly activated complexes of **1a** with two equivalents of samarium(II) are too demanding for DFT calculations at appropriate level.
[63] The terms "carbonyl first" and "alkene first" were employed by Procter, Flowers and Skrydstrup (see ref. 4) for samarium diiodide-promoted carbonyl-alkene couplings in order to classify the interaction of the electron transfer reagent with the substrates.
[64] For selected recent theoretical studies of samarium(II) halides including solvation effects, see: a) A. Ramírez-Solís, J. L. Amaro-Estrada, J. Hernández-Cobos, L. Maron, *J. Phys. Chem.* **2017**, *121*, 2293–2297; b) A. Ramírez-Solís, C. O. Bartulovich, T. V. Chciuk, J. Hernández-Cobos, H. Saint-Martin, L. Maron, W. R. Anderson, Jr., A. M. Li, R. A. Flowers II *J. Am. Chem. Soc.* **2018**, *140*, 16731–16739; c) J. Moon, H- Baek, J. Kim, *Mol. Phys.* **2019**, *117*, 241–250; d) A. Yamamoto, X. Liu, K. Arashiba, A. Konomi, H. Tanaka, K. Yoshizawa, Y. Nishibayashi, H. Yoshida, *Inorg. Chem.* **2023**, *62*, 5348–5356; e) J. Himmelstrup, V. R. Jensen, *J. Phys. Chem. A* **2023**, *127*, 3796–3805.
[65] Selected reviews dealing with synthetic applications of dearomatizing processes: a) L. N. Mander, *Synlett* **1991**, 134–144; b) F. L. Ortiz, M. J. Iglesias, I. Fernández, C. M. A. Sánchez, G. R. Gómez, *Chem. Rev.* **2007**, *107*, 1580–1691; c) S. P. Roche, J. A. Porco, *Angew. Chem. Int. Ed.* **2011**, *50*, 4068–4093; *Angew. Chem.* **2011**, *123*, 4154–4179; d) C.-X. Zhuo, C. Zheng, S.-L. You, *Acc. Chem. Res.* **2014**, *47*, 2558–2573; e) X. Just-Baringo, D. J. Procter, *Acc. Chem. Res.* **2015**, *48*, 1263–1275; f) W. C. Wertjes, E. M. Southgate, D. Sarlah, *Chem. Soc. Rev.* **2018**, *47*, 7996–8017; g) S.-L. You, *Chem. Soc. Rev.* **2020**, *49*, 286–300; h) C. Zheng, S.-L. You, *ACS Cent. Sci.* **2021**, *7*, 432–e444; i) N. Li, Z. Shi, W.-Z. Wang, Y. Yuan, K.-E. Ye, *Chem. Asian J.* **2023**, *18*, e202300122.
[66] R. Ahlrichs, M. Bär, M. Häser, H. Horn, C. Kölmel, *Chem. Phys. Lett.* **1989**, *162*, 165–169.
[67] J. P. Perdew, K. Burke, M. Ernzerhof, *Phys. Rev. Lett.* **1996**, *77*, 3865–3868.
[68] J. P. Perdew, M. Ernzerhof, K. Burke, *J. Chem. Phys.* **1996**, *105*, 9982–9985.
[69] S. Grimme, J. Antony, S. Ehrlich, H. Krieg, *J. Chem. Phys.* **2010**, *132*, 154104.
[70] S. Grimme, S. Ehrlich, L. Goerigk, *J. Comput. Chem.* **2011**, *32*, 1456–1465.
[71] M. Dolg, H. Stoll, A. Savin, H. Preuss, *Theor. Chim. Acta* **1989**, *75*, 173–194.
[72] F. Weigend, R. Ahlrichs, *Phys. Chem. Chem. Phys.* **2005**, *7*, 3297–3305.
[73] A. Klamt, G. Schürmann, *J. Chem. Soc. Perkin Trans. 2* **1993**, 799–805.
[74] A. Schäfer, A. Klamt, D. Sattel, J. C. Lohrenz, F. Eckert, *Phys. Chem. Chem. Phys.* **2000**, *2*, 2187–2193.
[75] S. Grimme, *Chem. Eur. J.* **2012**, *18*, 9955–9964.

Manuscript received: March 20, 2024
Accepted manuscript online: March 21, 2024
Version of record online: April 19, 2024